

Phonon-polaritons in Cu halides: Anomalies and their temperature dependence

Z. Vardeny* and O. Brafman

Department of Physics and Solid State Institute, Technion-Israel Institute of Technology, Haifa, Israel

(Received 7 August 1979)

The polariton Raman spectra of CuCl, CuBr, and CuI crystals are studied at various temperatures of their zinc-blende phase. Two polar modes are proven to exist in CuCl at room temperature and below; their oscillator-strength ratio changes with temperature and follows the temperature dependence of the lattice constant. In CuBr also two polar modes were observed at 300 and 80 K, but not at 2 K. In the latter case their oscillator-strength ratio shows an exponential temperature dependence. The two polar modes and their oscillator-strength temperature dependence are explained, assuming a temperature-dependent secondary minimum in the potential energy of the copper ion. Polariton spectra of CuI at room temperature and below show just one polar mode and behave regularly.

I. INTRODUCTION

The aim of this report is to present the polariton measurements in CuCl, CuBr, and CuI at various temperatures of interest and to offer an explanation for the phenomena observed and their temperature dependence.

Information on polaritons in Cu halides has been previously published on CuCl at 80 K^{1,2} and on CuI at room temperature.³ In the first report¹ on the polaritons in CuCl a theoretical fit could not be obtained with what seemed to be a normal polariton dispersion. In the second report² on the polaritons in CuCl more polariton branches were observed and the data were interpreted in terms of a Fermi resonance between the TO phonon and two peaks in the two-phonon density of states. The CuI polariton spectra show no irregularities³ and fit well the calculated dispersion curves.³

The purpose of the present report is to give more complete information on the polariton dispersion in this family of compounds and the way it changes with temperature. Both the polariton dispersion and its temperature dependence will be explained by a model previously proposed to explain many of the Cu-halide known anomalies.^{4,5}

We are dealing with the zinc-blende phase of CuCl, CuBr, and CuI with two atoms per primitive unit cell. Group theory predicts just one polar mode in this structure, and therefore two polariton branches are expected theoretically, of which only the lower one can be observed by the near-forward Raman-scattering technique.⁶ However, it is well known that in CuCl two TO-like modes appear in both its Raman^{4,7,8} and infrared spectra.⁹⁻¹¹ These lines were labeled⁷ β and γ . The γ line is relatively narrow and its corresponding LO(γ) is of about the same width, while TO(β) is much broader^{4,8} and the inability to assign a corresponding LO(β) remained a puzzle for quite

some time.⁴

In previous publications,^{4,5} a detailed review was given of the many anomalies found in CuCl, which were manifested in Bragg x-ray and neutron scattering, Raman scattering, infrared absorption and reflection, and neutron inelastic scattering. It was argued at length that all these anomalies can be interpreted in terms of secondary (off-center) minima in the potential energy of the copper ion.⁴ A dynamical model was assumed in which a Cu ion may populate its ideal position or four equivalent off-center sites located on the [111] directions toward the four faces of the tetrahedron formed by the anions—the quantum-mechanical tunneling states are formed of all five positions. The relative Cu⁺ population at central and off-center sites, depends on Δ , the energy difference between the corresponding potential energy minima. The magnitude of Δ is a function of the lattice parameter which is temperature and pressure dependent.

According to this model,⁴ two polar modes can exist: one in which Cu⁺ at ideal sites participate (γ) and the other in which Cu⁺ at off-center sites participate (β). Both modes, β and γ , exhibit the same Γ_{15} symmetry. The larger width of the β line is explained by a shorter correlation length of this mode. Within this interpretation the LO(β) line is to be found between TO(β) and TO(γ). In fact, all four lines [TO(β, γ), LO(β, γ)] were clearly reported at 2 K in Fig. 1 of Ref. 4. Polariton measurements are important to establish the nature of the β line: measure its dispersion, determine its oscillator strength, and also find out whether the line assigned as LO(β) shows any dispersion at all. Other than that not much has been expected of the polariton measurements of CuCl at different temperatures.

As interesting as it sounds for CuCl, it seemed even more important to measure the polariton

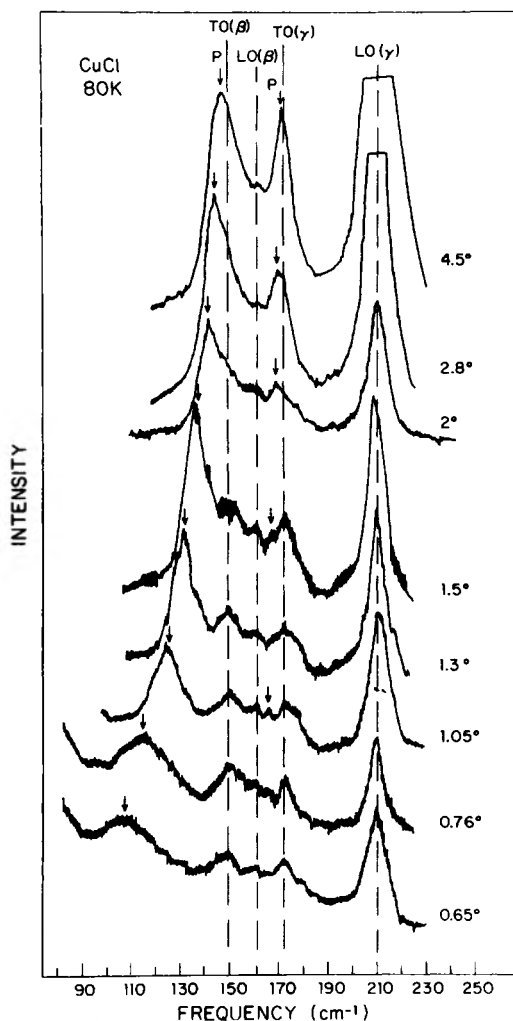


FIG. 1. Polariton spectra of CuCl at 80 K and various external angles ψ . The arrows mark the polariton frequencies, the vertical lines at $\omega_{TO(\beta)}$, $\omega_{LO(\beta)}$, $\omega_{TO(\gamma)}$, and $\omega_{LO(\gamma)}$ are drawn for reference.

dispersion in CuBr and at various temperatures. The situation in CuBr is more confusing because of the fewer experiments that have been performed on this compound.^{12,13} The model mentioned above⁴ claims a trend from CuCl to CuI and argues that a second polar mode does exist in CuBr as well as in CuCl. This other mode is not resolved in infrared.¹⁴ It is resolved in Raman at the 80–250 K temperature range,¹⁵ but its intensity temperature dependence resembles that of a difference combination of phonons rather than that of a first-order phonon.¹³ This intensity temperature dependence of the β -phonon line in CuBr was explained⁴ by the change of Δ (and therefore the Cu off-center population) as a result of the variation of the lattice parameter with temperature. The importance of recording the polariton spectra in

CuBr is therefore first of all to determine whether the extra mode β is really polar, and if so, to find out its oscillator strength. The temperature dependence of the polariton dispersion is then essential for the understanding of the origin and the nature of this phonon mode.

For the sake of completeness the CuI polariton dispersion was also measured in spite of the fact that no anomalies have been found concerning its polar mode, at room temperature and below,^{13,16} and although the room-temperature polariton spectra have already been reported.³ The experimental set up is described in Sec. II. In Sec. III the results and their interpretation are given for each compound at different temperatures. A general discussion is presented in Sec. IV and a summary in Sec. V.

II. EXPERIMENTAL

The near-forward-scattering spectra were excited by a Kr⁺ laser at its 6471-Å line with power of about 400 mW. The scattered light was analyzed using a triple spectrometer set for a resolution of 3–5 cm⁻¹ depending on the particular spectrum quality. We note that the width of the exit slit of the third monochromator was set at about the same width as those of the double monochromator. All three monochromators were operated in tandem for the frequency range measured. The laser beam was focused onto the sample using a long-focal-length (130-cm) lens to minimize the angular spread of the incident radiation. The Cu-halide crystals studied were in their zinc-blende phase, which justifies the use of a concentric annulus in order to restrict the opening angle of the collected scattered light.⁶ The scattering angle ψ (measured outside the crystal) was determined by the annulus radius and by its distance from the sample. Measurements were taken at angles in the range $0.4^\circ \leq \psi \leq 4.5^\circ$ with $\Delta\psi/\psi \approx \frac{1}{4}$. A scattering geometry in which \vec{e}_i is perpendicular to \vec{e}_s was preferred in each case in order to reduce ghost intensity. Immersion and cold-finger-type cryostats were used for measurements at 2 and 80 K, respectively.

The samples were kindly provided to us by I. P. Kaminow of Bell Telephone Laboratories. These were oriented single crystals with typical dimensions of a few mm and were extra-fine polished.

III. RESULTS AND INTERPRETATION

A. Cuprous chloride

(i) CuCl 80 K

Near-forward Raman-scattering spectra at 80 K are shown in Fig. 1 for various scattering angles

ψ . Straight lines are drawn for reference at the frequencies 149 cm^{-1} , 161 cm^{-1} , 173 cm^{-1} , and 210 cm^{-1} , corresponding to the frequencies of $\text{TO}(\beta)$, $\text{LO}(\beta)$, $\text{TO}(\gamma)$, and $\text{LO}(\gamma)$ phonons, respectively.⁴ The longitudinal modes $\text{LO}(\beta)$ and $\text{LO}(\gamma)$ are dispersionless and the peaks at $\omega_{\text{TO}}(\beta)$ and $\omega_{\text{TO}}(\gamma)$ are due to back-reflected scattering.⁶ The small arrows mark the β and γ polariton lines, the only lines whose frequencies change with ψ . The relative intensity of the γ polariton becomes smaller at smaller angles, but its width does not change significantly with ψ . The relative intensity and the width of the β polariton, on the other hand, enhances considerably at smaller ψ .

The polariton wave vector \bar{q} is calculated from the relation^{4,6}

$$q^2 = (\partial k / \partial \omega)^2 \omega_p(q)^2 + k_i k_s \psi^2 \quad (1)$$

(in units of energy), where $\partial k / \partial \omega = |n(\lambda) - \lambda \partial n / \partial \lambda|_L$ and $n(\lambda)$ is taken from the data of Ref. 17, \bar{k}_i and \bar{k}_s are the photon wave vectors of the incident and scattered radiation, respectively. The measured values of the polariton dispersion $\omega_p(q)$, are presented in Fig. 2. The measured frequencies of $\text{LO}(\beta)$ and $\text{LO}(\gamma)$ are also indicated in this figure in order to demonstrate their dispersionless nature.

The polariton dispersion is calculated from

$$cq = \omega [\epsilon(\omega)]^{1/2}. \quad (2)$$

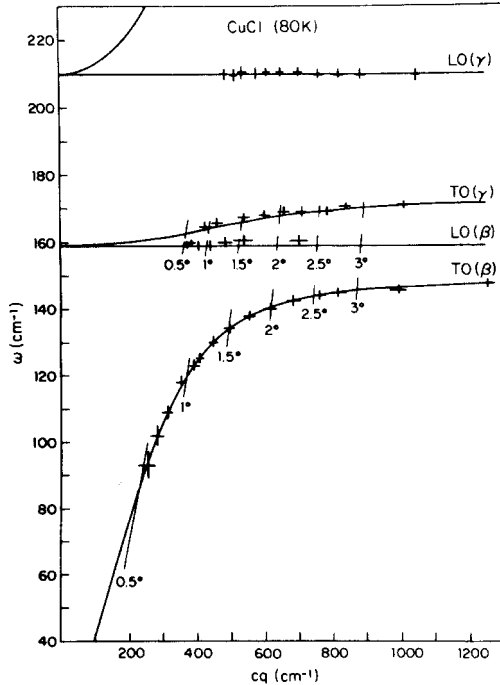


FIG. 2. Polariton dispersion in CuCl at 80 K. The full lines are the calculated best fit (see text) to the experimental data crosses.

When damping is excluded

$$\epsilon(\omega) = \epsilon(\infty) + \sum_j S_j / (1 - \omega^2 / \omega_j^2), \quad (3)$$

where S_j and ω_j are the strength and frequency of the j th polar mode. Usually, S_j is determined from infrared data, but in the case of CuCl, the different infrared measurements⁹⁻¹¹ yielded different S_j values. Instead, we preferred to use a single-parameter fit. The mode $\text{LO}(\gamma)$ is far from the rest of the lines and therefore the condition $\epsilon(\omega_{\text{LO}}(\gamma)) = 0$ holds, especially at low temperatures; this can also be derived from the infrared spectra.⁹⁻¹¹ With this condition and using $\epsilon(\infty) = 3.61$ from Ref. 1, S_β / S_γ is chosen as a parameter with which the data is best fitted and S_β and S_γ are obtained individually from Eq. (3). The best fit to the experimental results is obtained with $S_\beta / S_\gamma = 1.4 \pm 0.3$, and $S_\beta = 1.4 \pm 0.2$, $S_\gamma = 1.0 \pm 0.1$; this is shown in Fig. 2. $\epsilon_0 = \epsilon_\infty + S_\beta + S_\gamma = 6.1 \pm 0.1$ is derived from the polariton measurements and is in excellent agreement with the value of $\epsilon_0 = 6.1 \pm 0.1$ measured at 80 K.⁸ Moreover, the second zero of $\epsilon(\omega)$ is now calculated to be at $\omega_{\text{LO}}(\beta) = 159 \pm 1 \text{ cm}^{-1}$ compared with $\omega_{\text{LO}}(\beta) = 161 \pm 2 \text{ cm}^{-1}$ as read from the polariton spectra. With this value the (Lyddane-Sachs-Teller) LST relation which is written as

$$\epsilon_0 / \epsilon_\infty = [\omega_{\text{LO}}(\beta) \omega_{\text{LO}}(\gamma) / \omega_{\text{TO}}(\beta) \omega_{\text{TO}}(\gamma)]^2 \quad (4)$$

is perfectly obeyed.

There is also an alternative way to calculate the dispersion curves without fitting the S_β / S_γ ratio but rather determining it from the reduced Raman intensity ratio of the β and γ TO lines at large scattering angles.

For polar modes the reduced Raman-scattering intensity can be written as¹⁸

$$I_R / [n(\omega) + 1] = A(\omega) \epsilon''(\omega), \quad (5)$$

where I_R is the measured Raman intensity, $A(\omega)$ is the Raman matrix element, n is the Bose Einstein factor, and $\epsilon''(\omega)$ is the imaginary part of the dielectric function. For velocity damped harmonic oscillators¹⁸

$$\epsilon''(\omega) = \sum_j \epsilon_\infty S_j \omega \gamma_j \omega_j^2 [(\omega_j^2 - \omega^2)^2 + (\omega \gamma_j)^2]. \quad (6)$$

Assuming $A(\omega(\beta)) \approx A(\omega(\gamma))$, the reduced intensity ratio⁴ of β and γ modes yields $S_\beta / S_\gamma \approx 1.8$, which is within the range of values obtained by fitting the polariton data. This result shows that the assumption $A(\omega(\beta)) \approx A(\omega(\gamma))$ can be used to a fair approximation. Of course one should not ignore the inaccuracy in measuring the intensities of the $\text{TO}(\beta)$ and $\text{TO}(\gamma)$ lines, especially because of the third line, $\text{LO}(\beta)$, lying in between. Another ver-

ification of the present conclusion of two oscillators contributing to $\epsilon(\omega)$ of CuCl at 80 K comes from the polariton relative intensity measurements.

For cubic crystals, the frequency-dependent Raman intensity $I(\omega)$, without damping, is written as²

$$I(\omega) = C\omega^2 \left(\sum \frac{a_j \omega_j S_j^{1/2}}{\omega_j^2 - \omega^2} + 4\pi b \right)^2 / \left(\epsilon_\infty + \sum \frac{S_j}{(1 - \omega^2/\omega_j^2)^2} \right), \quad (7)$$

where a^j is the j th mode atomic displacement tensor, b is the electro-optic tensor element, and C is a normalization factor. At the j th frequency $I(\omega) \sim |a^j|^2$, thus the individual relative $|a^j|^2$ values can be derived from the reduced Raman-scattering intensities at large ψ . Using also the intensity of a longitudinal mode [$I_{LO}(\gamma)$ in the case of CuCl], two sets of equations for the relative b parameter can be obtained.^{6,19} For CuCl with $\lambda_L = 6471 \text{ \AA}$, $I_{TO}(\beta)/I_{TO}(\gamma) = 1.8$, and $I_{LO}(\gamma)/I_{TO}(\gamma) = 2.3$ and the two solutions calculated have opposite signs of b/a^j . In general, for frequencies lower than ω_{TO} , when $b/a > 0$ the polariton intensity enhances,^{19,20} and when $b/a < 0$ the polariton intensity decreases when ψ decreases. The right sign of b/a only can be chosen experimentally.

The relative intensities of the β and γ polaritons were measured in each spectrum and the β reflected back scattering intensity was used for the calibration of the polariton intensity at the different angles.²¹ The experimental results are presented in Fig. 3; naturally the errors involved in these values are quite substantial, but nevertheless, the fit to the calculated $I(\omega)$ with $b/a < 0$ is remarkably good. The solution using $b/a > 0$ has no similarity whatsoever to the experimental results and is not shown.

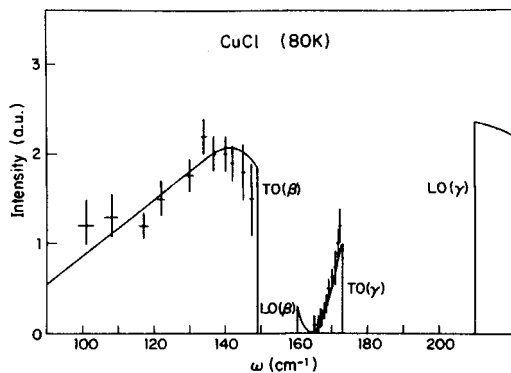


FIG. 3. Frequency-dependent intensity of CuCl at 80 K: calculated—full line, experimental—crosses.

$I_{LO}(\beta)$ was not taken as a fixed parameter in the calculation of $I(\omega)$, but its calculated intensity agrees very well with its measured intensity at large ψ ; $I_{LO}(\beta)/I_{TO}(\beta) = 0.2$ and was derived from the excess of intensity in the β mode (which appears as an asymmetry at the high-frequency side of the β peak).² This fact supports the procedure *a posteriori*, and also the assignment of the line as $LO(\beta)$. Furthermore, it may explain the smaller ratio of $I_{LO}(\beta)/I_{TO}(\gamma) = 0.2$, compared to $I_{LO}(\gamma)/I_{TO}(\gamma) = 2.3$ which holds at 80 K.

In two previous reports, the polariton spectra of CuCl at 80 K^{1,2} are described. In the first one¹ the $TO(\gamma)$ dispersion was not observed and thus the attempt to fit the data to a single oscillator was unsuccessful. In the second report² the $TO(\gamma)$ dispersion has indeed been measured, but the data were interpreted in terms of a Fermi resonance between $TO(\gamma)$ and two peaks in the combined two-phonon density of states, $g_{\pm}^2(\omega)$: $\omega = 141 \text{ cm}^{-1}$ and $\omega = 162 \text{ cm}^{-1}$. In this model² $S_1, S_2 \ll S(\gamma)$ and it is required that ω_2 will be dispersive. $\omega_2 \approx \omega_{LO}(\beta)$ and we have shown that this line is dispersionless. Moreover, at $\psi = 4.5^\circ$ the frequency of the β polariton approaches 148 cm^{-1} , which is a lot higher than the ω_1 frequency (141 cm^{-1}). Also the LST relation is not obeyed with the Fermi resonance interpretation. The small S_1 and S_2 values do not give the correct $\epsilon_0 = \epsilon_\infty + \sum_j S_j$ value. Equivalently, these S_1 and S_2 yield $\omega_{LO}(1) = 142 \text{ cm}^{-1}$ and $\omega_{LO}(2) = 163 \text{ cm}^{-1}$, and therefore

$$\epsilon_0(\text{LST}) = \epsilon_\infty [\omega_{LO}(1)\omega_{LO}(2)\omega_{LO}(\gamma)]^2 / [\omega_{TO}(1)\omega_{TO}(2) \times \omega_{TO}(\gamma)]^2 = 5.6,$$

compared to $\epsilon_0 = 6.1$ measured^{7,8} at 80 K.

(ii) CuCl 300 K.

The dispersion of the γ polariton in CuCl is small at 80 K and is expected to be considerably larger at 300 K. On the other hand, the Raman lines are much wider due to the large anharmonicity of the crystal. From Fig. 4, it is clear that in spite of the very broad lines, it is possible to measure the polariton dispersion in CuCl even at 300 K.

The polariton lines are marked by small arrows and the straight lines are drawn at the frequencies $\omega_{TO}(\beta) = 123 \text{ cm}^{-1}$, $\omega_{LO}(\beta) = 139 \text{ cm}^{-1}$, $\omega_{TO}(\gamma) = 162 \text{ cm}^{-1}$, and $\omega_{LO}(\gamma) = 202 \text{ cm}^{-1}$. The dispersion of the γ polariton is clearly more pronounced than that recorded at 80 K, but the width of all the lines, especially those of the polaritons, are by far larger. The measured shift of the γ polariton frequency is 14 cm^{-1} compared with 7 cm^{-1} measured at 80 K. The experimental $\omega_p(q)$ values of both the polaritons and the LO lines are shown in

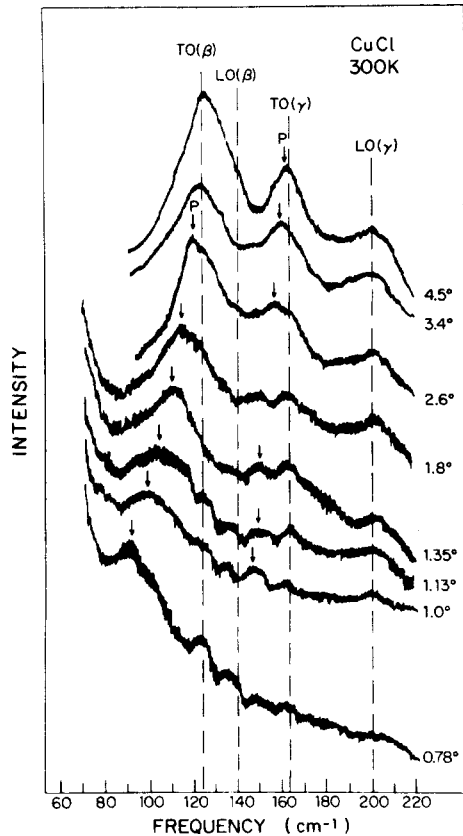


FIG. 4. Polariton spectra of CuCl at 300 K (compare with Fig. 1).

Fig. 5.

The LO(β) line is placed between two wide and intense lines [(TO(β) and TO(γ)] at room temperature and therefore was not noticed in the large angle Raman scattering. Only in the thesis of Prevot,²² a trace of LO(β) seem to have been observed when LO allowed geometry was used [$z(xy)z$]. At near-forward-scattering geometry, as opposed to the back-reflected part, the forward scattering part of the TO(β) line shifts to lower frequencies, leaving a weaker reflected back scattering trace. On the other hand, the LO(β) line is dispersionless and therefore its line intensity consists of both forward scattering and back-reflected intensities. At angles sufficiently small ($\psi \leq 1.3^\circ$) LO(β) is indeed detected and its frequency is $139 \pm 3 \text{ cm}^{-1}$ (Fig. 4).

At 300 K, the lines of CuCl are broad and it may seem oversimplified to calculate the polariton dispersion using an undamped $\epsilon(\omega)$ function. Nevertheless, from the work of Rimai *et al.*²³ it turns out that the undamped oscillator can be considered as a reasonable approximation unless the width of the line is comparable to its frequency. However, when an attempt is made to calculate the

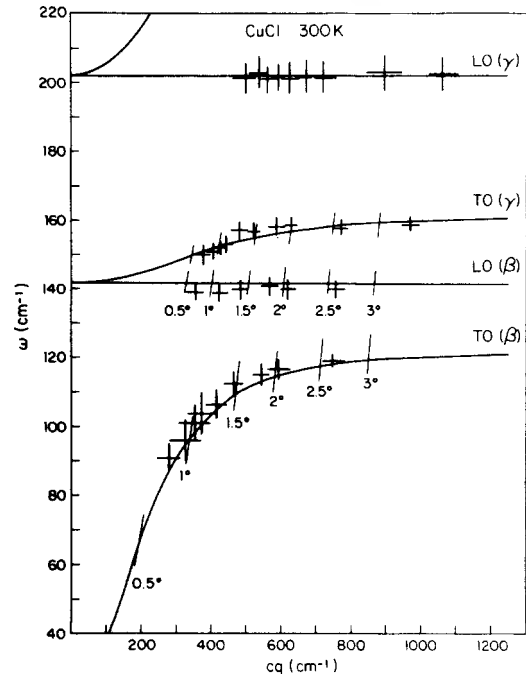


FIG. 5. Polariton dispersion in CuCl at 300 K. The full lines are the calculated best fit (see text) to the experimental data crosses.

dispersion curves following the procedure used for the 80 K case, two difficulties arise. From infrared data^{11,14} at 300 K it is obvious that $\epsilon(\omega_{\text{LO}}(\gamma)) \neq 0$, and in addition the LO(γ) line is very wide. For these reasons, in order to fit the data $\omega_{\text{LO}}(\gamma)$ was allowed to vary in accordance with the experimental frequency uncertainty: $\omega_{\text{LO}}(\gamma) = 200 \pm 5 \text{ cm}^{-1}$, this in addition to the parameter S_β/S_γ . It should also be noted that because of the broad lines, the inaccuracy in the data points is rather large (Fig. 4). The best fit shown in Fig. 5 was obtained with $S_\beta/S_\gamma = 2.5 \pm 0.5$, $S_\beta = 2.8 \pm 0.4$, $S_\gamma = 1.1 \pm 0.1$. With these values $\epsilon_0 = \epsilon_\infty + S_\beta + S_\gamma = 7.5 \pm 0.5$ is obtained, which fits fairly well the measured^{7,8} $\epsilon_0 = 7.9 \pm 0.5$ at 300 K. The second zero of $\epsilon(\omega)$ comes out at $142 \pm 2 \text{ cm}^{-1}$ compared with $139 \pm 2 \text{ cm}^{-1}$ which is the observed LO(β) frequency. Clearly, the second zero and the LO(β) frequency do not have to coincide; the same arguments given above for LO(γ) hold at least as well for LO(β).

B. Cuprous bromide

It was generally accepted^{12,13,15} that there is nothing anomalous about the Raman spectra of CuBr, although it was known that the wide line observed at room temperature consists of two lines.¹³ These lines are unresolved in infrared,¹⁴ and therefore their individual oscillator strengths

are unknown. Moreover, the intensity temperature dependence of one of the lines is higher than that of a first-order phonon line, and therefore this line (β) was considered to be a difference combination,^{12,13,15} especially because it vanishes¹⁵ at 2 K.

It was our assertion⁴ that the anomalies found in CuCl are not unique and that there is a trend in the Cu halides anomalous properties, increasing from CuI to CuCl. We find that the polariton data of CuBr is of special importance as far as the mode of Cu⁺ at off-center sites is concerned. The Cu⁺ off-center population in CuBr is highly sensitive to temperature variation unlike CuCl.⁴ The individual oscillator strengths of β and γ at various temperatures can be deduced from the polaritons dispersion and thus shed more light on the mechanism involved.

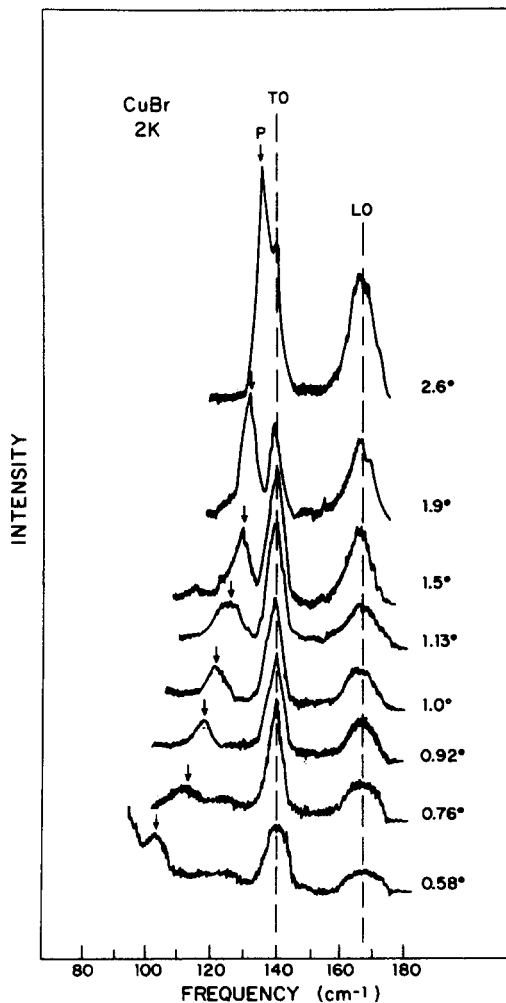


FIG. 6. Polariton spectra of CuBr at 2 K for several external scattering angles ψ . The polariton lines are marked by arrows, the vertical lines at $\omega_{\text{TO}}(\gamma)$ and $\omega_{\text{LO}}(\gamma)$ are drawn for reference.

(i) CuBr 2 K

The near-forward Raman spectra at 2 K for several external scattering angles are shown in Fig. 6. The straight lines are drawn at $\omega_{\text{TO}}(\gamma) = 140 \text{ cm}^{-1}$ and $\omega_{\text{LO}}(\gamma) = 169 \text{ cm}^{-1}$. Only a single polariton mode is observed; its width increases and its relative intensity decreases for decreasing ψ . The rest of the lines in the spectra are the back-reflected TO and the dispersionless LO mode.

The polariton wave vectors were calculated using Eq. (1) and the values of $n(\lambda)$ and $|n - \lambda \partial n / \partial \lambda|_L$ taken from Refs. 12 and 17. It is worthwhile to mention that at 6471 \AA , the value of $|n - \lambda \partial n / \partial \lambda|_L$ is quite small and theoretically the full branch of the lower polariton is measurable. This can be seen in Fig. 7 where the experimental $\omega_p(q)$ data are shown.

The theoretical curve was calculated using a single oscillator with a strength

$$S = (\omega_{\text{LO}}^2 / \omega_{\text{TO}}^2 - 1) \epsilon_{\infty}. \quad (8)$$

Taking¹² $\epsilon_{\infty} = 4.06$, $\omega_{\text{LO}}(\gamma) = 169 \text{ cm}^{-1}$, $\omega_{\text{TO}}(\gamma) = 140 \text{ cm}^{-1}$, one gets $S = 1.86$. With this value the theoretical curve matches perfectly the experimental results. This means that at 2 K, just one mode contributes to $\epsilon(\omega)$, the γ mode.

The frequency-dependent intensity $I(\omega)$ was calculated using Eq. (7) for a single oscillator and $I_{\text{LO}}/I_{\text{TO}} = 2$ at 6471 \AA and large ψ . The two possible solutions of $I(\omega)$ are shown in Fig. 8: $I_1(\omega)$ —

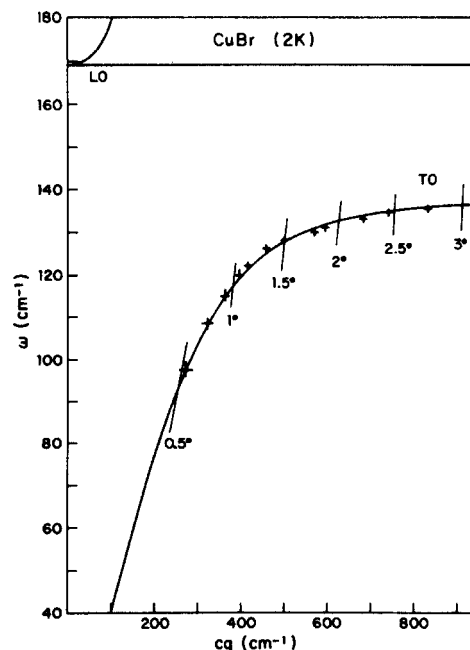


FIG. 7. Polariton dispersion in CuBr at 2 K: full line—theoretical curve, crosses—experimental values.

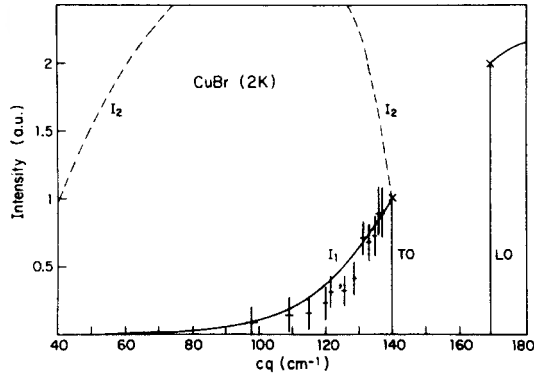


FIG. 8. Experimental $I(\omega)$ values of CuBr at 2 K compared with the calculated $I_1(\omega)$ ($b/a < 0$) and $I_2(\omega)$ ($b/a > 0$), see text.

based on $b/a < 0$ and $I_2(\omega)$ —based on $b/a > 0$. The comparison with the experimental results obviously proves that $b/a < 0$ in CuBr just as in CuCl.

(ii) CuBr 80 K

In CuBr spectra at 80 K the two modes β and γ are well resolved as is demonstrated in Fig. 9: $\omega_{\text{TO}}(\beta) = 121 \text{ cm}^{-1}$ and $\omega_{\text{TO}}(\gamma) = 138 \text{ cm}^{-1}$, $\omega_{\text{LO}}(\gamma) = 169 \text{ cm}^{-1}$. Definitely two polariton modes β and γ are observed. The frequency of the γ polariton reaches almost $\omega(\beta)$, its relative intensity decreases while it narrows at small ψ . On the other hand, the intensity and width of the β polariton increase when ψ decreases. This is the first experimental evidence of the existence of the β - γ anomaly in CuBr, i.e., both lines are infrared active and thus belong to the same representation Γ_{15} .

The experimental $\omega_p(q)$ data are shown in Fig. 10. For the theoretical dispersion curves, a best-fit procedure was carried out exactly the way it was done for CuCl for 80 K: the ratio S_β/S_γ was taken as a fitting parameter with the constraint that $\epsilon(\omega_{\text{LO}}(\gamma)) = 0$. The excellent fit shown in Fig. 10 was obtained with the ratio $S_\beta/S_\gamma = \frac{1}{6}$. The ratio between the reduced Raman intensities of β and γ is around the same value; this ratio is hard to estimate because of the low intensity of the β mode at this temperature. The individual oscillator strengths $S_\beta = 0.3 \pm 0.2$ and $S_\gamma = 1.85 \pm 0.05$ are then calculated. Using these values $\epsilon_0 = \epsilon_\infty + S_\beta + S_\gamma = 6.2 \pm 0.15$ and fits very well the measured value of $\epsilon_0 = 6.2$ at 80 K.¹² The second zero of $\epsilon(\omega)$ comes out at $122.5 \pm 0.5 \text{ cm}^{-1}$ and it is very close to $\omega_{\text{TO}}(\beta)$ (121 cm^{-1}); this might be the reason that no LO-TO splitting of the β mode could be detected. The calculated polariton dispersion curves based on the single oscillator γ ($138, 169 \text{ cm}^{-1}$) are also shown in Fig. 10, in order to

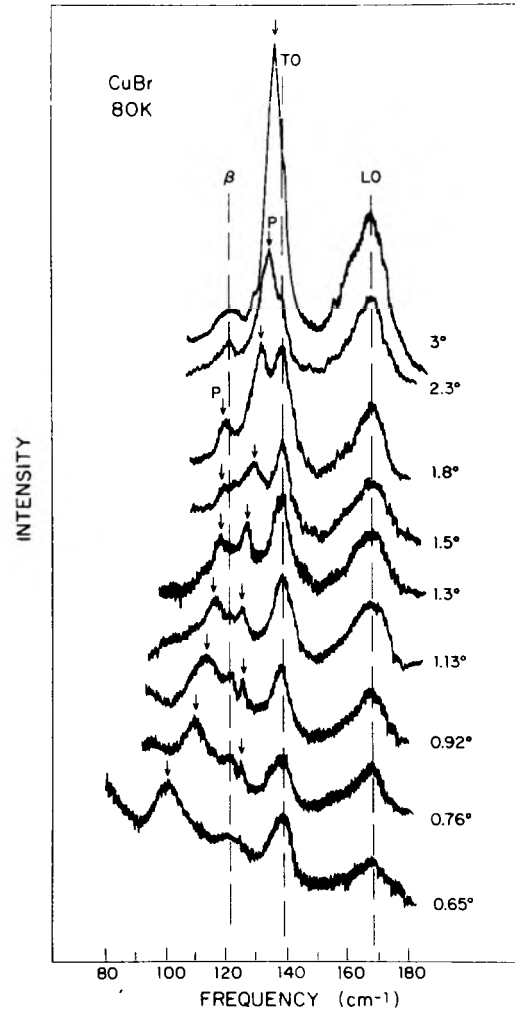


FIG. 9. Polariton spectra of CuBr at 80 K for several angles ψ . The arrows mark the polariton lines. The vertical lines at $\omega(\beta)$, $\omega_{\text{TO}}(\gamma)$, and $\omega_{\text{LO}}(\gamma)$ are drawn for reference.

demonstrate their disagreement with the polariton measured data.

The dispersion of the γ polariton decreases at small wave vectors (Fig. 10) and this explains its narrowing at small ψ (Fig. 9). The behavior differs from that characteristic of a lower polariton branch, which broadens at smaller wave vectors.⁶ This fact supports our conclusion: γ is not the lower polariton branch in this case. Two modes contribute to $\epsilon(\omega)$ of CuBr at 80 K so that the γ polariton can shift down to a frequency as low as $\omega_{\text{LO}}(\beta)$ (see Fig. 10).

The fit obtained between the experimental and calculated $I(\omega)$ shown in Fig. 11 further supports this conclusion. $I(\omega)$ was calculated using Eq. (7) and $I_{\text{TO}}(\beta)/I_{\text{TO}}(\gamma) = \frac{1}{6}$, $I_{\text{LO}}(\gamma)/I_{\text{TO}}(\gamma) = 2$. The results obtained at 2 K prescribe the solution for

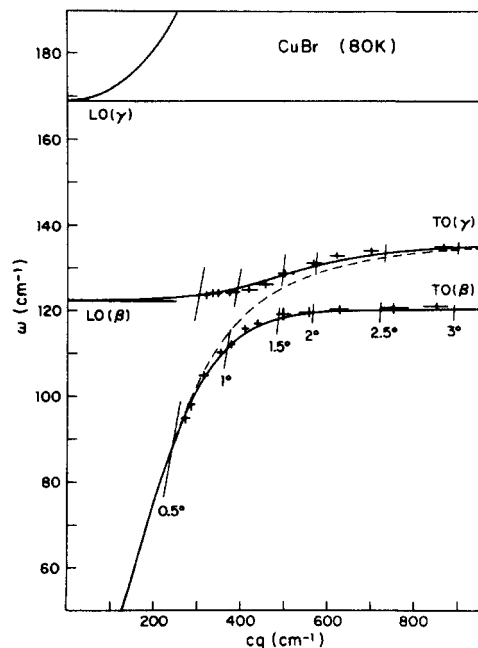


FIG. 10. Polariton dispersion in CuBr at 80 K. The full lines are the calculated best fit (see text) to the experimental data crosses. The dashed line is the calculated polariton dispersion based on a single oscillator (γ).

which $b/a < 0$. The fit to the calculated $I(\omega)$ based on the two oscillators β and γ is excellent, taking into account the large experimental uncertainties. On the other hand, $I(\omega)$ based on a single oscillator (γ), which is also shown in Fig. 11, clearly disagrees with the experimental results. It is worthwhile to mention that the calculated $I(\omega_{LO(\beta)})$ is negligibly small and this also explains the inability to detect this line even at small scattering angles, where it is more likely to be detected.

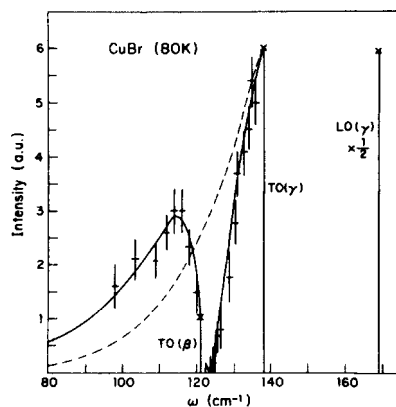


FIG. 11. Experimental $I(\omega)$ values of CuBr at 80 K compared with the calculated $I(\omega)$ based on two oscillators β and γ (full line) and the calculated $I(\omega)$ based on a single γ oscillator (dashed line).

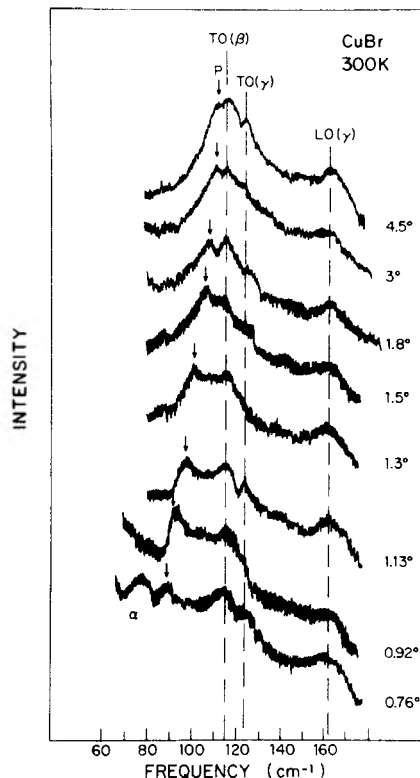


FIG. 12. Polariton spectra of CuBr at 300 K (compare with Fig. 9).

(iii) CuBr 300 K

The β mode becomes much more dispersive at 300 K, where at large ψ its Raman line is more intense than that of the γ mode. In Fig. 12 the CuBr polariton spectra at room temperature are shown essentially to demonstrate that contrary to the case of CuCl at 300 K, well defined polaritons are recorded here, in spite of the large width of the β - γ peak at large ψ . At room temperature $\omega_{TO(\beta)} = 114 \text{ cm}^{-1}$, $\omega_{TO(\gamma)} = 124 \text{ cm}^{-1}$, and $\omega_{LO(\gamma)} = 163 \text{ cm}^{-1}$ (Refs. 4, 12, 13), but $TO(\beta)$ and $TO(\gamma)$ are unresolved. Therefore only the β polariton can be detected. If at 80 K, because of the small S_β/S_γ ratio, a resonance interaction between the higher γ polariton and the β mode could be considered, it certainly can not be the case of room temperature where the β polariton is well observed even at rather large ψ , which means that its oscillator strength is large.

In order to evaluate the β and γ oscillator strengths, again S_β/S_γ was chosen as a fitting parameter together with the relation $\epsilon(\omega_{LO(\gamma)}) = 0$. The best fit between the calculated dispersion curves and the experimental data is shown in Fig. 13 and was obtained with $S_\beta/S_\gamma = 2$, $S_\beta \approx 2.5 \pm 0.4$, and $S_\gamma \approx 1.2 \pm 0.2$. These values yield $\epsilon_0 = 7.8 \pm 0.3$

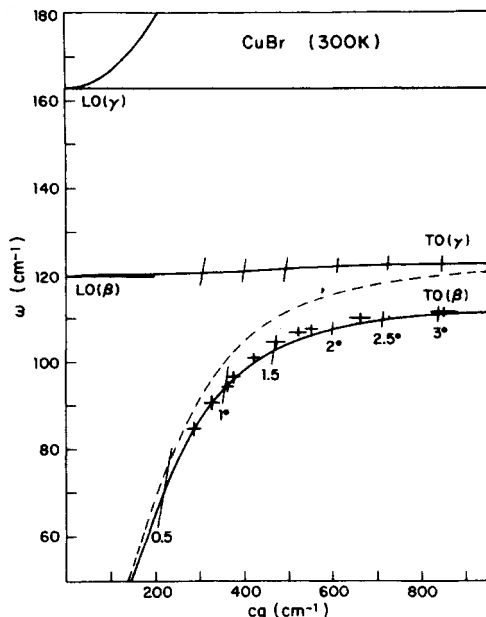


FIG. 13. Polariton dispersion in CuBr at 300 K. The full lines are the calculated best fit (see text) to the experimental data crosses. The dashed line is the calculated polariton dispersion based on a single oscillator (γ).

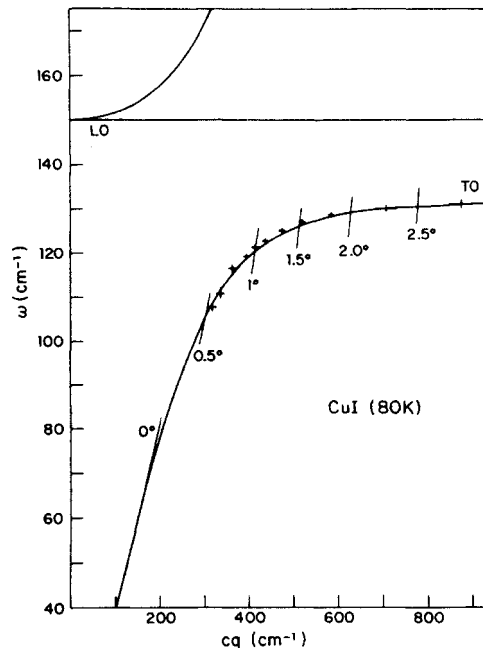


FIG. 15. Polariton dispersion of CuI at 80 K. Crosses represent the measured values and the full lines are the theoretical dispersion curves.

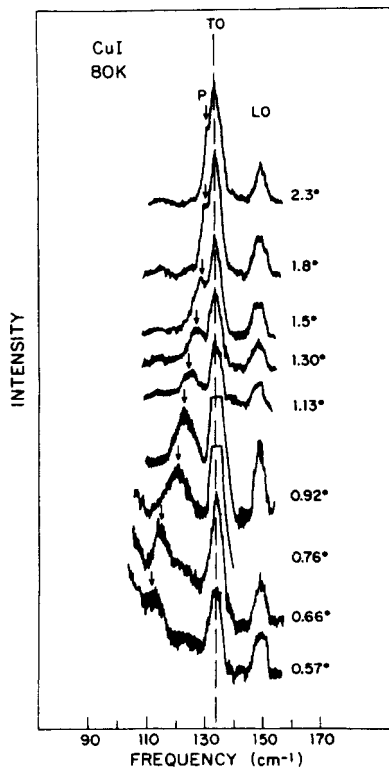


FIG. 14. Polariton spectra of CuI at 80 K for several external angles ψ . The polariton lines are marked by arrows, the vertical lines at $\omega_{TO}(\gamma)$ and $\omega_{LO}(\gamma)$ are drawn for reference.

as compared to $\epsilon_0 = 7.9 \pm 0.4$ measured at room temperature.¹² The second zero of $\epsilon(\omega)$ is determined to be at 119 ± 2 cm^{-1} , which is in between the wide lines of $TO(\beta)$ and $TO(\gamma)$ and therefore could not be detected even at small ψ . With this value of $\omega_{LO}(\beta)$ the LST relation [Eq. (4)] is perfectly obeyed.⁴

For comparison, the dispersion curve based on a single oscillator γ (124, 163 cm^{-1}) is also shown in Fig. 13, but clearly does not fit the experimental results. Also the LST relation based on the single oscillator γ is not obeyed.⁴ There is no possibility of meaningfully measuring the polariton intensities at 300 K.

C. CuI

The polariton spectra of CuI were recorded for the sake of completeness only. Anomalies of the kind found in CuCl and CuBr were not found in CuI at $T < 500$ K,¹⁶ but at high temperatures polariton measurements are more complicated. Our measurements at 300 K confirm those reported by Wiener-Avneer,³ except that we were able to record a much larger shift of the polariton frequency when excited by longer-wavelength radiation.

The nearly-forward Raman-scattering spectra at 80 K for several angles ψ are shown in Fig. 14. With $\epsilon_\infty = 4.84$,¹³ $\omega_{TO} = 133$ cm^{-1} , and $\omega_{LO} = 150$ cm^{-1} one gets [Eq. (8)] $S = 1.27$. Figure 15 shows the

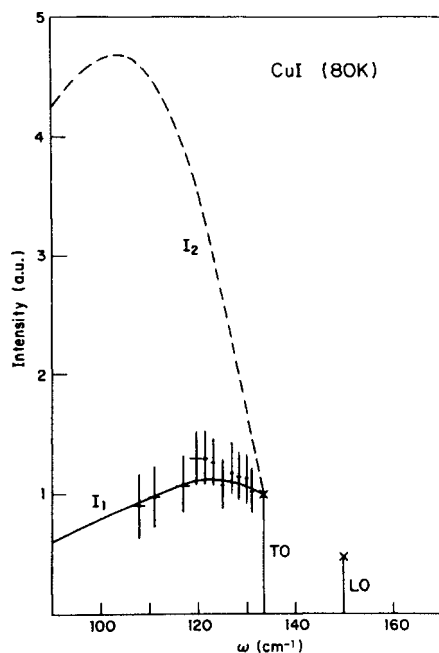


FIG. 16. Calculated (full line) and experimental (crosses) $I(\omega)$ for CuI at 80 K.

excellent fit between the calculated polariton dispersion curves and the experimental results. $I(\omega)$ was calculated using $I_{LO}/I_{TO} = 0.45$. Again, only $I_1(\omega)$ for which $b/a < 0$ fits the measured polariton relative intensities, as is shown in Fig. 16.

IV. GENERAL DISCUSSION

As a matter of principle whenever the infrared data can yield sufficiently accurate oscillator strengths, the polariton dispersion curves can readily be calculated. In that case measuring polariton dispersion may be considered as a double check only, or as a measure of the degree of the infrared accuracy.

There is a number of reports on infrared measurements^{9-11,14} of CuCl, but these yield different oscillator-strength values. However, they do agree upon the basic question, namely, the existence of two oscillators of considerable strength at all temperatures. Nevertheless, the previous

TABLE I. The oscillator strength of the β and γ modes in CuCl and the measured $(\epsilon_0 - \epsilon_\infty)_{\text{expt}} = S_\beta + S_\gamma$ at different temperatures.

$T(K)$	S_β	S_γ	S_β/S_γ	$(\epsilon_0 - \epsilon_\infty)_{\text{expt}}$
2	1.7 ^a	0.6 ^a	2.8 ^a	2.3
80	1.4	1	1.4	2.5
300	2.8	1.1	2.5	4.3

^a Reference 24.

two reports^{1,2} on polaritons in CuCl ignored these results. In one,¹ an attempt was made to fit the polariton data by a single oscillator and in the other altogether three oscillators were assumed: a Fermi resonance of the TO mode with two multiphonon modes.²

In the present report a good fit to *two* oscillators was obtained and it should be looked upon as a supporting evidence of the fact established by infrared data. At least at low temperature we regard the oscillator-strength values determined from polariton measurements to be more accurate than those yielded by infrared measurements.

In Table I a summary is given of the CuCl oscillator strength of the β and γ modes determined from the polariton measurements at 2 (Ref. 24), 80, and 300 K. The sum of S_β and S_γ should be compared with the measured values of $\epsilon_0 - \epsilon_\infty$. The fit is remarkable at 2 and 80 K. The good fit obtained at 300 K may be misleading, regarding the very broad lines of CuCl at this temperature (see Fig. 4). The column S_β/S_γ of Table I is of special importance. One of the arguments in the model⁴ to explain the existence of a second oscillator at very low T in CuCl is based on the negative thermal expansion coefficient²⁵ of CuCl below 100 K; the off-center Cu^+ potential well deepens at low temperatures,⁴ and consequently the off-center Cu^+ population increases. The ratio of the β - γ oscillator strengths can be regarded as a measure of the ratio between the off-center population and that of the center, respectively. It is clear that roughly speaking this ratio follows nicely the temperature changes of the lattice parameter, which has a minimum of about 100 K.

In order to understand the physics of CuBr, the polariton measurements proving the existence of two oscillators at 80 and 300 K, are absolutely necessary. These two oscillators are very close in energy and could not be resolved in infrared.¹⁴

In fact at 300 K these lines were hardly resolved in Raman scattering⁴ and at 80 K the intensity of the β line is small compared to that of the γ line.¹⁵ Because of its Raman intensity temperature dependence, the additional β line was believed to be a difference band^{12,13,15} and as such was ignored

TABLE II. The oscillator strength of the β and γ modes in CuBr and the measured $(\epsilon_0 - \epsilon_\infty)_{\text{expt}} = S_\beta + S_\gamma$ at different temperatures.

$T(K)$	S_β	S_γ	S_β/S_γ	$(\epsilon_0 - \epsilon_\infty)_{\text{expt}}$
2	0	1.9	0	
80	0.3	1.9	0.18	2.2
300	2.5	1.2	2.0	3.8

altogether. The proof that both β and γ are polar modes comes solely from the polariton measurements, which in addition yield information about their oscillator strengths. This information is summarized in Table II where their relative strengths are given at different temperatures. Assuming that Δ itself does not change much with temperature in CuBr, Δ can be calculated with the help of S_β/S_γ at 80 and 300 K given in Table II, and assuming an exponential behavior of this ratio with temperature, this calculation yields Δ of the order of 200 K, which does seem reasonable owing to the fact that S_γ does not change significantly between 2 and 80 K. It is therefore concluded that at very low temperatures Cu⁺ are at the ideal positions and the off-center-to-center population ratio increases rapidly with temperature.

Our polariton-dispersion measurements of CuCl, CuBr and CuI show that in CuCl two oscillators exist at all temperatures, in CuBr the second oscillator disappears at very low temperatures, while in CuI just one oscillator is observed at temperatures lower than 300 K. This trend in the Cu-halide crystals is one of the basic features of our model.⁴

V. SUMMARY

The polariton spectra of CuCl, CuBr, and CuI at various temperatures were presented and dis-

cussed. The measured $\omega_p(q)$ values were fitted by a calculation based on two oscillators in CuCl at all temperatures, two oscillators in CuBr at 300 and 80K, but only one oscillator at 2 K and just one oscillator in CuI at 300 K and below. Also the frequency-dependent polariton intensities support the same conclusions. The intensity fit shows that in these crystals $b/a < 0$ as is the case for all known zinc-blende materials.

The anomalous existence of two polar modes in a structure which theoretically allows for a single polar mode only, is explained by the irregular behavior of the copper ion. The assumption that Cu⁺ occupies its ideal site or four equivalent off-center sites explains the appearance of an extra polar mode. Moreover, the oscillator-strength ratio as function of temperature also fits within this framework; there is a correlation between the expected ratio of the Cu⁺ off-center and central population and the derived oscillator-strength ratio of the corresponding β and γ modes.

ACKNOWLEDGMENTS

We are grateful to I. P. Kaminow of Bell Telephone Laboratories for supplying us the single crystals of Cu halides. We thank H. Katz for skillful technical assistance and M. Mor for expert polishing of the crystals.

*This work was done in partial fulfillment of the requirements for the Ph.D. degree. Present address: Division of Engineering, Brown University, Providence, Rhode Island 02912.

¹M. L. Shand, L. Y. Ching, and E. Burstein, *Solid State Commun.* **15**, 1209 (1974).

²K. Fukushi, M. Nippus, and R. Claus, *Phys. Status Solidi B* **86**, 257 (1978).

³E. Wiener-Avneer, *Phys. Status Solidi B* **75**, 717 (1976).

⁴Z. Vardeny and O. Brafman, *Phys. Rev. B* **19**, 3276 (1979).

⁵Z. Vardeny and O. Brafman, *Phys. Rev. B* **19**, 3290 (1979).

⁶R. Claus, L. Merten, and J. Brandmüller, *Springer Tracts Mod. Phys.* **75** (1975).

⁷I. P. Kaminow and E. H. Turner, *Phys. Rev. B* **5**, 1564 (1972).

⁸J. E. Potts, R. C. Hanson, C. J. Walker, and C. Schwab, *Phys. Rev. B* **9**, 2711 (1974).

⁹M. Ikezawa, *J. Phys. Soc. Jpn.* **35**, 309 (1973).

¹⁰A. Hadni, F. Brehat, J. Claudel, and P. Strimer, *J. Chem. Phys.* **49**, 471 (1968).

¹¹N. Plendl and L. C. Mansur, *Appl. Opt.* **11**, 1194 (1972).

¹²E. M. Turner, I. P. Kaminow, and C. Schwab, *Phys. Rev. B* **9**, 2524 (1974).

¹³J. E. Potts, R. C. Hanson, and C. T. Walker, *Solid*

State Commun. **13**, 389 (1973).

¹⁴J. N. Plendl, A. Hadni, J. Claudel, Y. Henninger, G. Morlot, P. Strimer, and L. C. Mansur, *Appl. Opt.* **5**, 397 (1966).

¹⁵T. Fukumoto, S. Nakashima, K. Tabuchi, and A. Mitsui, *Phys. Status Solidi B* **73**, 341 (1976).

¹⁶G. Burns, F. H. Dacol, and W. M. Shafer, *Solid State Commun.* **24**, 753 (1977).

¹⁷A. Feldman and D. Horowitz, *J. Opt. Soc. Am.* **59**, 1406 (1969).

¹⁸G. Burns, F. H. Dacol, M. W. Shafer, *Phys. Rev. B* **16**, 1416 (1977).

¹⁹S. Ushioda, A. Pinczuk, W. Taylor, and E. Burstein, *Proceedings of the International Conference on Semiconductor Compounds*, edited by D. G. Thomas (Benjamin, New York, 1967).

²⁰J. A. Freitas, J. M. Nicola, and R. C. C. Leite, *Solid State Commun.* **25**, 65 (1978).

²¹B. Prevot, Ph.D. thesis, Strasburg, 1976 (unpublished).

²²L. Rimai, J. L. Parsons, J. T. Hichmott, and T. Nakamura, *Phys. Rev.* **168**, 623 (1968).

²³The polariton spectra of CuCl at 2 K will be reported elsewhere in connection with CuCl_xBr_{1-x}.

²⁴T. H. K. Barron, J. A. Birch, and G. K. White, *J. Phys. C* **10**, 1617 (1977).